

## Exploration of the internal cavity of histone deacetylase (HDAC) with selective HDAC1/HDAC2 inhibitors (SHI-1:2)

Joey L. Methot,<sup>a,\*</sup> Prasun K. Chakravarty,<sup>d</sup> Melissa Chenard,<sup>c</sup> Joshua Close,<sup>a</sup>  
Jonathan C. Cruz,<sup>c</sup> William K. Dahlberg,<sup>a</sup> Judith Fleming,<sup>b</sup>  
Christopher L. Hamblett,<sup>a</sup> Julie E. Hamill,<sup>a</sup> Paul Harrington,<sup>a,†</sup> Andreas Harsch,<sup>a</sup>  
Richard Heidebrecht,<sup>a</sup> Bethany Hughes,<sup>a</sup> Joon Jung,<sup>a</sup> Candia M. Kenific,<sup>c</sup>  
Astrid M. Kral,<sup>b</sup> Peter T. Meinke,<sup>d</sup> Richard E. Middleton,<sup>a</sup> Nicole Ozerova,<sup>b</sup>  
David L. Sloman,<sup>a</sup> Matthew G. Stanton,<sup>a</sup> Alexander A. Szewczak,<sup>a</sup>  
Sriram Tyagarajan,<sup>d</sup> David J. Witter,<sup>a</sup> J. Paul Secrist<sup>b</sup> and Thomas A. Miller<sup>a</sup>

<sup>a</sup>Department of Drug Design and Optimization, Merck Research Laboratories, 33 Avenue Louis Pasteur, Boston, MA 02115, USA

<sup>b</sup>Department of Cancer Biology and Therapeutics, Merck Research Laboratories, 33 Avenue Louis Pasteur, Boston, MA 02115, USA

<sup>c</sup>Department of Oncology and Pharmacology, Merck Research Laboratories, 33 Avenue Louis Pasteur, Boston, MA 02115, USA

<sup>d</sup>Department of Medicinal Chemistry, Merck Research Laboratories, 126 E. Lincoln Avenue, Rahway, NJ 07065, USA

Received 21 November 2007; revised 11 December 2007; accepted 13 December 2007

Available online 7 January 2008

**Abstract**—We report herein the initial exploration of novel selective HDAC1/HDAC2 inhibitors (SHI-1:2). Optimized SHI-1:2 structures exhibit enhanced intrinsic activity against HDAC1 and HDAC2, and are greater than 100-fold selective versus other HDACs, including HDAC3. Based on the SAR of these agents and our current understanding of the HDAC active site, we postulate that the SHI-1:2 extend the existing HDAC inhibitor pharmacophore to include an internal binding domain.

© 2008 Elsevier Ltd. All rights reserved.

The histone deacetylase (HDAC) family of metalloenzymes is extensively involved in epigenetic regulation of gene expression.<sup>1</sup> They catalyze the cleavage of the *N*-acetyl group from acetylated lysine residues located on the tails of the core nucleosomal histones H2a, H2b, H3, and H4. However overexpression of histone deacetylase leads to hypoacetylated chromatin that becomes inaccessible to transcription factors, for example. These enzymes also regulate the acetylation status of numerous nonhistone proteins such as transcription factors p53, STAT1, and NF- $\kappa$ B as well as  $\alpha$ -tubulin, Hsp90, and Ku70.<sup>2</sup>

There are 11 zinc-dependent HDAC enzymes characterized to date, divided into three classes. Class I enzymes

(HDACs 1–3 and 8) are 350–500 amino acids in length, are ubiquitously expressed, and are located primarily in the nucleus. Class II enzymes (HDACs 4–7, 9 and 10) are about 1000 amino acids in length, are tissue-specific, and can shuttle between the cytoplasm and the nucleus. HDAC11 contains residues common to both classes and also has tissue-specific expression; and is considered the only class IV HDAC. Seven additional *NAD*-dependent HDACs comprise Class III. Known as SIRT1–7, this silencing information regulator 2 (Sir2) family of deacetylases has a unique catalytic mechanism that requires the cofactor nicotinamide adenine dinucleotide and these enzymes respond to changes in cellular redox.<sup>3</sup>

Small molecule inhibitors<sup>4</sup> of histone deacetylase have been shown to activate transcription of genes regulating cell-cycle progression, differentiation, and/or apoptosis in cancer cells and these agents generally conform to a broadly accepted pharmacophore. In late 2006, Zolinza<sup>TM</sup> became the first HDAC inhibitor to gain FDA approval and is used for the treatment of the cutaneous manifestations of T-cell lymphoma (Fig. 1).<sup>5</sup> Like many

**Keywords:** HDAC inhibitor; Isoform selectivity; HDAC3; Internal cavity; Biaryl.

\* Corresponding author. Tel.: +1 617 992 2054; fax: +1 617 992 2403; e-mail: [joey\\_methot@merck.com](mailto:joey_methot@merck.com)

<sup>†</sup> Present address: Department of Medicinal Chemistry, Amgen Inc., One Amgen Center Drive, Thousand Oaks, CA 91320-1799, USA.

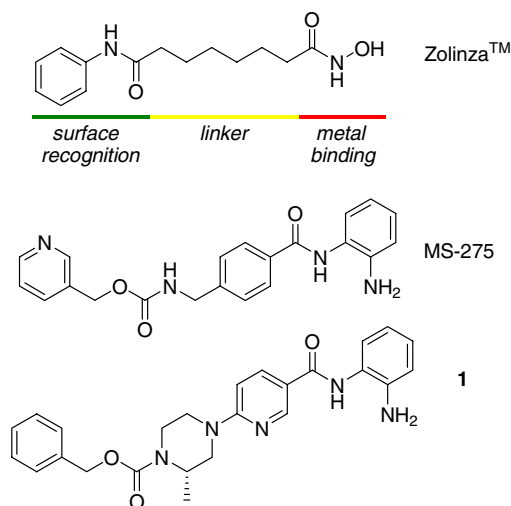


**Figure 1.** HDAC inhibitors Zolinza™, MS-275, and piperazyl benzamide **1**.

inhibitors containing a hydroxamic acid moiety in the zinc-binding motif, Zolinza™ (SAHA, vorinostat) is a broad-spectrum HDAC inhibitor. Another class of HDAC inhibitors contains an  $\alpha$ -aminobenzamide zinc-binding motif as exemplified by MS-275<sup>6</sup> (SNDX-275) and nicotinyl piperazine **1**.<sup>7</sup> As is typically observed for benzamide-derived inhibitors, compound **1** inhibits HDACs 1–3 but does not significantly inhibit the other HDAC isoforms screened. Though the histone deacetylase family is well documented in the development of cancer, the role of the individual HDACs remains unclear. HDACs 1 and 2 share a high degree of homology and are found in the same multicomponent nuclear complexes containing transcriptional co-repressors such as mSin3 and NuRD.<sup>8</sup> They both have been shown to be overexpressed in human cancers and knockdown leads to increased apoptosis.<sup>9</sup>

Distinct from HDACs 1 and 2, HDAC3 is found in the NCoR-SMRT co-repressor complex. The physiological role of HDAC3 is less well understood, though it is overexpressed in certain colon tumors<sup>10</sup> and it is capable of interacting with the class II HDACs as a functional link between the classes. For example, the activity of HDACs 4, 5, and 7 has been shown to be dependent on HDAC3.<sup>11</sup> In a recent study using DNA microarrays, Zolinza™ was found to activate or repress the expression of at least 22% of genes in a 16-h cell culture, most of which are involved in cell proliferation and apoptotic pathways.<sup>12</sup> Hence, isoform-selective inhibitors would help our understanding of the individual roles of the HDAC family, and may even offer an improved therapeutic window by modulating a small set of disease-focused genes.<sup>13</sup>

As part of our efforts to further improve the selectivity of benzamides such as **1**, we investigated potent and selective hydroxybiphenyl benzamide **2**, which was discovered through an HTS campaign (Fig. 2).<sup>14</sup> Benzamide **2**, and closely related analogs, were prepared previously as part of a program directed toward the

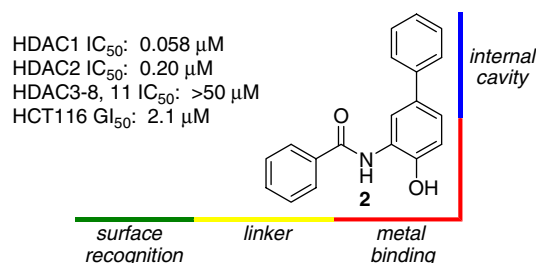


**Figure 2.** A biaryl benzamide imparts >100-fold selectivity for HDACs 1 and 2 versus HDAC3. The new pharmacophore model places the pendant phenyl ring into the internal cavity.

identification of potential antiprotozoal agents using total nuclear HDAC activity as a screening tool.<sup>15</sup> Despite lacking a surface recognition domain, compound **2** exhibits good potency in HDAC1 and HDAC2 biochemical activity assays (IC<sub>50</sub> 0.058 and 0.20  $\mu$ M, respectively).<sup>16</sup> Most notably, **2** is inactive against all other HDAC isoforms screened, including HDACs 3–8 and 11. In an HCT116 human colon carcinoma cell viability assay, **2** exhibits promising antiproliferative activity (GI<sub>50</sub> 2.1  $\mu$ M).<sup>17</sup> The lack of HDAC3 activity exhibited by these biaryl benzamides is in striking contrast to simple benzamides such as **1**. Herein we focus on the influence of substituents putatively residing in the internal cavity domain.

A small library of amide derivatives was prepared holding the hydroxybiphenylaniline constant (Table 1). The HDAC1 inhibition data parallel the SAR of the phenylenediamine-derived benzamide inhibitors lacking the pendant aryl substituent (data not shown). The 2-pyridyl analog was not well tolerated; however 3-pyridyl

**Table 1.** Exploration of the amide moiety of biaryl phenol **2**

Compound	Substituent R	HDAC1 IC <sub>50</sub> ( $\mu$ M)
<b>2</b>	Phenyl	0.058
<b>3</b>	2-Pyridyl	0.31
<b>4</b>	3-Pyridyl	0.068
<b>5</b>	4-Pyridyl	0.075
<b>6</b>	2-Thiophenyl	0.13
<b>7</b>	2-Benzothiophenyl	0.13
<b>8</b>	2-Benzothiazolyl	0.35
<b>9</b>	2-Furanyl	0.13
<b>10</b>	5-Isoxazolyl	0.10
<b>11</b>	2-Aminophenyl	1.8
<b>12</b>	3-Aminophenyl	0.44
<b>13</b>	4-Aminophenyl	0.040
<b>14</b>	Acetyl	4.8
<b>15</b>	Benzyl	>50
<b>16</b>	Hydrocinnamyl	0.61
<b>17</b>	Cinnamyl	1.2
<b>18</b>	Acetoxy	>50
<b>19</b>	Benzyloxy	>50

and 4-pyridyl analogs were found to be equipotent to **2**, with HDAC1 IC<sub>50</sub> values of 0.068 and 0.075  $\mu$ M, respectively. Thiophene, benzothiophene, furan, and isoxazole ring (**6**, **7**, **9**, and **10**) replacements were found to be acceptable, with less than a twofold loss in potency, although the 2-benzothiazolyl analog was found to be sub-optimal. An amino substituent placed on the benzoyl group of **2** was well tolerated at the *para*-position (**13**), but not at the *ortho*- or *meta*-positions. Nonaryl amides **14–17** were at least one log unit less potent than **2**, and lastly acetoxycarbamate and benzyloxy carbamate (**18** and **19**) were found to be inactive.

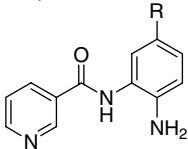
Given the structural homology between **2** and the clinical agent MS-275, we replaced the phenol of **2** with an aniline for subsequent studies. Following our research with nicotinoyl benzamides such as **1**, we also elected to further explore the SAR of biaryl moiety analogs containing the nicotinoyl moiety in the linker domain (Table 2). As a reference, *N*-(2-aminophenyl)-nicotinamide **20** inhibits HDAC1 with an IC<sub>50</sub> of 2.6  $\mu$ M. Installation of the pendant hydrophobic phenyl, 2-thiophene or 3-thiophene (**21–23**) characteristic of the SHI-1:2 structures gave a 50-fold boost in potency. Introduction of more polar groups such as 1-imidazolyl and 4-pyridyl led to a 15- to 20-fold loss in potency versus phenyl substituted **21**, while the 3,5-pyrazinyl derivative was inactive. We turned to nonaromatic substitution and were encouraged by pyrrolidine **28** (HDAC1 IC<sub>50</sub> 0.67  $\mu$ M). However analog **29**, having a cyclopentyl substituent, was sixfold less potent, and dimethylamine (**30**) and morpholinyl analogs (**31**) were inactive. Methyl and trifluoromethyl analogs are also inactive. These studies suggest that a small aromatic moiety is optimal for bind-

ing in the narrow entry to the internal cavity. Lastly, substitution with halides (**37** and **38**) led to inactivity; indicating polarity may be poorly tolerated in this region of the active site.

With phenyl biaryl **21** being among the most promising leads, we explored substitution about the pendant phenyl ring (internal cavity domain) (Table 3). Installation of a variety of groups at *ortho*- or *meta*-positions led to a dramatic loss in potency (data not shown), while substitution at the *para*-position is somewhat permitted. Substitution with a fluorine was allowed with little penalty, however aniline **40** was sevenfold less potent than **21** and dimethylaniline **41** was 100-fold less potent. A methyl nitrile substituent was permitted (**42**; HDAC1 IC<sub>50</sub> 0.25  $\mu$ M) however charged amine and carboxylic acid substituents (**43**, **44**, and **47**) were not. Interestingly, benzyl and methyl esters **45** and **48** were modestly potent (IC<sub>50</sub> values of 1.3–1.5  $\mu$ M), indicating that there is space in the internal cavity of HDAC1 for larger hydrophobic groups. Further exploration of the internal binding domain revealed that insertion of oxygen, carbonyl, ethyl or piperazinyl linkers is not tolerated (Table 4).

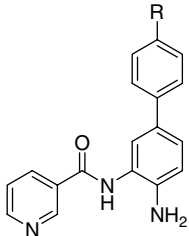
Summarized in Table 5 are the HDAC isoform biochemical and HCT116 human colon carcinoma cell proliferative activities of nicotinoyl leads **21** and **22** and the analogous benzoyl leads **54** and **55**. As we have seen, *N*-(2-aminophenyl)nicotinamide **20** and the benzoyl analog **53** are modest inhibitors of HDAC1 with little selectivity over HDAC2 or HDAC3. The introduction of a phenyl or 2-thiophene substituent gives a 100-fold boost in HDAC1 potency (IC<sub>50</sub> 0.048–0.065  $\mu$ M). Selectivity over HDAC2 is >15-fold for the phenyl biaryls and >5-fold for the thiophenyl biaryls, and all biaryls are a remarkable selectivity of >100-fold over HDAC3. Benzamide inhibitors **20–22** and **53–55** do not significantly inhibit HDACs 4–8 or 11 (IC<sub>50</sub> >50  $\mu$ M).

Table 2. SAR of the nicotinyl aniline

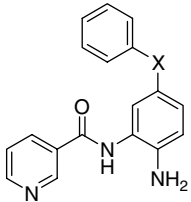


Compound	Substituent R	HDAC1 IC <sub>50</sub> ( $\mu$ M)
<b>20</b>	Hydrogen	2.6
<b>21</b>	Phenyl	0.048
<b>22</b>	2-Thiophenyl	0.065
<b>23</b>	3-Thiophenyl	0.052
<b>24</b>	3-Furanyl	0.16
<b>25</b>	1-Imidazolyl	1.0
<b>26</b>	4-Pyridyl	0.65
<b>27</b>	3,5-Pyrazyl	>50
<b>28</b>	1-Pyrrolidinyl	0.67
<b>29</b>	Cyclopentyl	4.2
<b>30</b>	Dimethylaminyl	44
<b>31</b>	Morpholinyl	>50
<b>32</b>	CO <sub>2</sub> H	>50
<b>33</b>	CO <sub>2</sub> Me	>50
<b>34</b>	CONHMe	>50
<b>35</b>	Methyl	>50
<b>36</b>	Trifluoromethyl	>50
<b>37</b>	Chlorine	>50
<b>38</b>	Fluorine	>50

Table 3. Derivatization of phenyl biaryl **21**



Compound	Substituent R	HDAC1 IC <sub>50</sub> ( $\mu$ M)
<b>21</b>	Hydrogen	0.048
<b>39</b>	Fluorine	0.14
<b>40</b>	NH <sub>2</sub>	0.33
<b>41</b>	NMe <sub>2</sub>	5.3
<b>42</b>	CH <sub>2</sub> CN	0.25
<b>43</b>	CH <sub>2</sub> NH <sub>2</sub>	2.1
<b>44</b>	CO <sub>2</sub> H	>50
<b>45</b>	CO <sub>2</sub> CH <sub>2</sub> Ph	1.3
<b>46</b>	C(O)-morpholine	>50
<b>47</b>	CH <sub>2</sub> CH <sub>2</sub> CO <sub>2</sub> H	13
<b>48</b>	CH <sub>2</sub> CH <sub>2</sub> CO <sub>2</sub> Me	1.5

**Table 4.** Introduction of a linker into biaryl **21**


Compound	Linker X	HDAC1 IC <sub>50</sub> (μM)
<b>21</b>	Bond	0.048
<b>49</b>	CO	>50
<b>50</b>	O	>50
<b>51</b>	Ethyl	>50
<b>52</b>	Piperazine	>50

**Table 5.** Summary of nicotiny and benzoyl biaryl leads

The chemical structure shows a benzamide derivative. A benzene ring is substituted with a linker 'X' at the para position and an amide group (-C(=O)NH-) at the other para position. The amide nitrogen is further substituted with a 4-amino-2-substituted phenyl group. The substituent 'R' is located at the 2-position of this second phenyl ring, which also has an amino group (-NH<sub>2</sub>) at the 4-position.

Compound	IC <sub>50</sub> (μM)			GI <sub>50</sub> HCT116 (μM)
	HDAC1	HDAC2	HDAC3	
<b>X=N</b>				
<b>20</b> : R = H	2.6	7.0	3.6	24
<b>21</b> : R = phenyl	0.048	0.90	11	2.1
<b>22</b> : R = 2-thiophenyl	0.065	0.39	7.3	2.4
<b>X=CH</b>				
<b>53</b> : R = H	2.4	3.3	2.8	21
<b>54</b> : R = phenyl	0.060	0.78	11	2.0
<b>55</b> : R = 2-thiophenyl	0.048	0.36	11	0.72

In 2004, Weist and co-workers postulated the role of the internal cavity adjacent to the zinc active site of histone deacetylase.<sup>18</sup> They put forth a proposal for an inhibitor design accessing this internal cavity with a new binding element. The binding of the zinc-binding motif of biaryl **21** is expected to be similar to simple benzamides such as **1**, however with a thiophene substituent directed into the internal cavity.

To address the selectivity of the biaryl SHI-1:2 class, we constructed homology models of HDACs 1 and 3 based on the 1.9-Å X-ray structure of an inactive mutant HDAC8 bound to an acetylated peptidic substrate.<sup>19</sup> The active sites of the class I HDACs are virtually identical. Overall homology between HDACs 1 and 8 is good, with 43% identical and 66% similar residues. Between HDACs 3 and 8, the homology is 43% identical and 64% similar residues. Likewise, the homology between HDACs 1 and 3 is very high 62% identical and 82% similar residues with one most notable exception; Ser113 in the internal cavity of HDAC1 is replaced by Tyr96 in HDAC3.

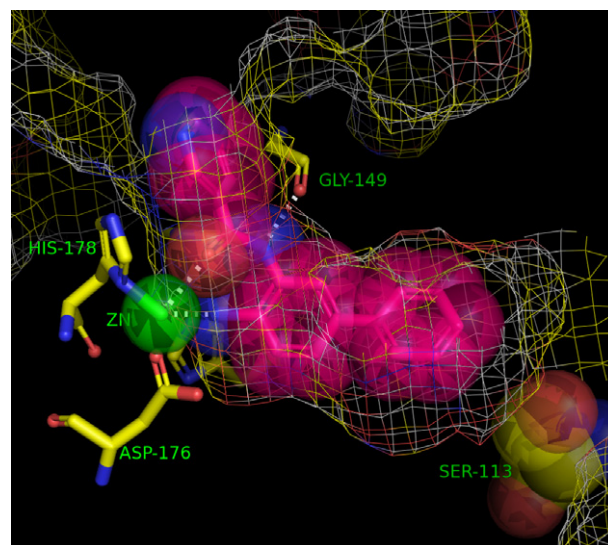
Shown in **Figure 3** is the active site model of HDAC1 docked with biphenyl lead **21**. The ball and stick representation shows the carbonyl and aniline groups bound to zinc (shown in green) while the N–H bonds to Gly149. The phenyl fits neatly into the internal cavity with a phenyl–phenyl dihedral angle of 35°; nearly equivalent to that measured from an energy minimization without enzyme. The space filling representation illustrates how little space there is available for substitution about the pendant phenyl ring.

We now can begin to understand the SAR outlined in **Table 2**. Given the hydrophobic character of the internal cavity, nonpolar substituents are preferred over polar groups such as imidazolyl, pyridyl or pyrazyl. Pyrrolidine **28** is likely able to adopt a near coplanar conformation with the benzamide, while cyclopentyl **29** cannot. Other alkyl substituents are likely too large. As seen in **Figure 3**, there is space within the internal cavity for substitution at the *para*-position of the biaryl (**Table 3**).

Putative binding of **21** to HDAC3 illustrates a potential source of SHI-1:2 selectivity (**Fig. 4**), wherein, tyrosine-96 replaces serine-113 in the lower corner of the internal cavity, completely blocking access of a biaryl.

After considerable investigation of the internal cavity domain, we opted to further explore analogs containing a nicotiny or benzoyl in the linker domain. For example, the biphenyl analog/hybrid of **1** and **2** shown in **Figure 5** is a potent, selective SHI-1:2. However, the HDAC1 inhibitory activity of **56** is not improved, and only a marginal improvement in the antiproliferative activity was observed. The poor solubility of **56** is likely the culprit.

Further optimization of the linker and recognition domains led to analogs of CI-994<sup>20</sup> (**Table 6**). CI-994 was a clinical agent with modest activity (HDAC1 IC<sub>50</sub> 0.57 μM), however incorporation of our biphenyl phenol or aniline resulted in a 20- to 30-fold boost in

**Figure 3.** Model of **21** bound to HDAC1.



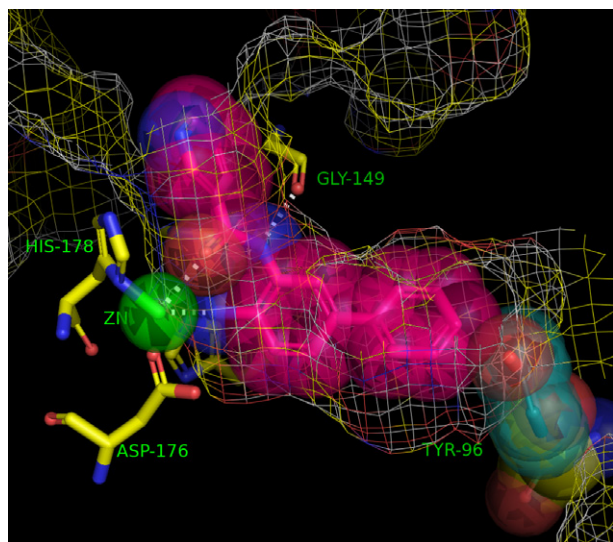


**Figure 4.** Putative model of **21** bound to HDAC3. The phenyl biaryl would overlap with tyrosine-96.

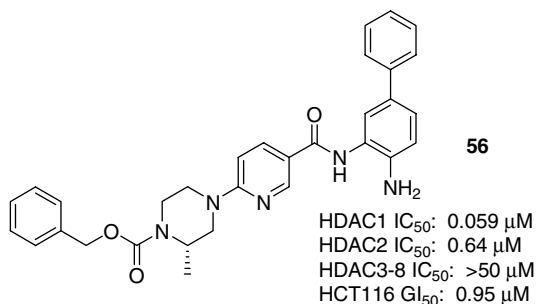


**Figure 5.** Biaryl analog of piperazine **2**.

**Table 6.** Biaryl analogs of CI-994

Compound	R <sup>1</sup>	R <sup>2</sup>	HDAC1 IC <sub>50</sub> ( $\mu$ M)
CI-994	NH <sub>2</sub>	H	0.57
<b>57</b>	OH	Ph	0.018
<b>58</b>	NH <sub>2</sub>	Ph	0.028
<b>59</b>	F	Ph	>50
<b>60</b>	NH <sub>2</sub>	2-Thiophene	0.007
<b>61</b>	NH <sub>2</sub>	3-Thiophene	0.007
<b>62</b>	NH <sub>2</sub>	CO <sub>2</sub> H	>50
<b>63</b>	NH <sub>2</sub>	CO <sub>2</sub> Me	4.5
<b>64</b>	NH <sub>2</sub>	CONHMe	>50
<b>65</b>	NH <sub>2</sub>	CONHPh	>50

potency. A fluorobiaryl (**59**) was inactive reaffirming the requirement of a strong chelate with zinc in the active site. The thiophene analogs **60** and **61** were remarkably potent inhibitors (IC<sub>50</sub> 7 nM), however once again the introduction of polar acid, ester or amide functional

groups led to an erosion in HDAC1 activity. Placement of the *N*-acetamide group at the *meta*-position gave a threefold loss in potency (data not shown).

2-Thiophenyl biaryl **60** also exhibits potent HDAC2 inhibitory activity (IC<sub>50</sub> 0.049  $\mu$ M), is selective versus other HDAC isoforms (IC<sub>50</sub>  $\geq$  10  $\mu$ M), and is potent in the HCT116 proliferation assay (GI<sub>50</sub> 0.11  $\mu$ M). Compound **60** is devoid of CYP (>50  $\mu$ M) and hERG (>30  $\mu$ M) activity, and has acceptable rat pharmacokinetics in both the iv (2 mg/kg dose; Cl 12 mL/min/kg; Vd<sub>ss</sub> 6.9 L/kg; *t*<sub>1/2</sub> 9.7 h) and po (4 mg/kg dose; AUC<sub>N</sub> 2.8  $\mu$ M h/mg/kg; *C*<sub>max</sub> 1.4  $\mu$ M; *F* 64%) arms.

Given these promising features, biaryl **60** was evaluated in an HCT116 mouse xenograft model of cancer (Fig. 6).<sup>21</sup> Gratifyingly, at a dose of 30 mg/kg administered ip the inhibitor was tolerated and a 52% tumor growth inhibition was observed without significant weight loss. However, as the dose was escalated to 45 and 60 mg/kg ip, adverse effects caused termination of the study by 10 and 8 days, respectively. Despite having a poor therapeutic margin, compound **60** represents a promising discovery lead. Inhibitors possessing an improved therapeutic index will be the focus of future disclosures.

The discovery of biaryl inhibitors such as phenol **2** and aniline **21** represents a new class of HDAC1 and HDAC2-selective tools, termed SHI-1:2, that may help clarify the roles of the individual class I HDACs in human cancer. SAR gathered to date indicates that the observed selectivity may arise from the orientation of the hydrophobic aryl substituent into the internal cavity of the HDAC enzymes, with preferential binding to HDAC1 over HDAC3. The SHI-1:2 class of HDAC inhibitors exhibit potent antiproliferative activity and inhibit tumor growth in a mouse xenograft model.

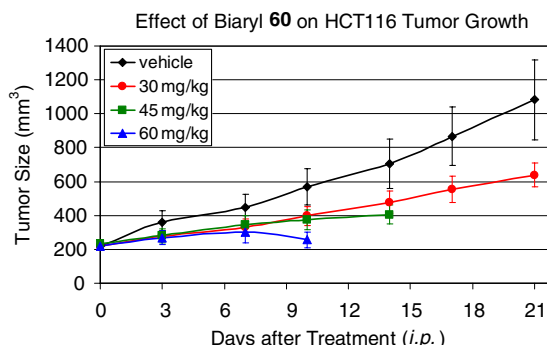
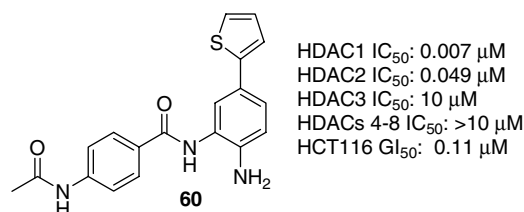


**Figure 6.** HCT116 xenograft mouse model efficacy study with 2-thiophenyl biaryl **60**.

Further studies of the SHI-1:2 will be the subject of future disclosures.

### References and notes

- Lund, A. H.; van Lohuizen, M. *Genes Dev.* **2004**, *18*, 2315.
- Bolden, J. E.; Peart, M. J.; Johnstone, R. W. *Nat. Rev. Drug Discov.* **2006**, *5*, 769.
- Blander, G.; Guarente, L. *Annu. Rev. Biochem.* **2004**, *73*, 417.
- Miller, T. A.; Witter, D. J.; Belvedere, S. *J. Med. Chem.* **2003**, *46*, 5097.
- (a) Richon, V. M. *Br. J. Cancer* **2006**, *95*, S2; (b) O'Connor, O. A. *Br. J. Cancer* **2006**, *95*, S7; (c) Duvic, M.; Zhang, C. *Br. J. Cancer* **2006**, *95*, S13; (d) Marks, P. A.; Breslow, R. *Nat. Biotechnol.* **2007**, *25*, 84.
- (a) Suzuki, T.; Ando, T.; Tsuchiya, K.; Fukazawa, N.; Saito, A.; Mariko, Y.; Yamashita, T.; Nakanishi, O. *J. Med. Chem.* **1999**, *42*, 3001; (b) Kell, J. *Curr. Opin. Invest. Drugs* **2007**, *8*, 485.
- Hamblett, C. L.; Methot, J. L.; Mampreian, D. M.; Sloman, D. L.; Stanton, M. G.; Kral, A. M.; Fleming, J. C.; Cruz, J. C.; Chenard, M.; Ozerova, N.; Hitz, A. M.; Wang, H.; Deshmukh, S. V.; Nazef, N.; Harsch, A.; Hughes, B.; Dahlberg, W. K.; Szewczak, A. A.; Middleton, R. E.; Mosley, R. T.; Secrist, J. P.; Miller, T. A. *Bioorg. Med. Chem. Lett.* **2007**, *17*, 5300.
- Knoepfler, P. S.; Eisenman, R. N. *Cell* **1999**, *99*, 447.
- (a) Lager, G.; O'Carroll, D.; Rembold, M.; Khier, H.; Tischler, J.; Weitzer, G. *EMBO J.* **2002**, *21*, 2672; (b) Huang, B. H.; Laban, M.; Leung, C. H.; Lee, L.; Lee, C. K.; Salto-Tellez, M. *Cell Death Differ.* **2005**, *12*, 395.
- Wilson, A. J.; Byun, D.-S.; Popova, N.; Murray, L. B.; L'Italien, K.; Sowa, Y.; Arango, D.; Velcich, A.; Augenlicht, L. H.; Mariadason, J. M. *J. Biol. Chem.* **2006**, *281*, 13548.
- (a) Grozinger, C. M.; Hassig, C. A.; Schreiber, S. L. *Proc. Natl. Acad. Sci. U.S.A.* **1999**, *96*, 4868; (b) Fischle, W.; Dequiedt, F.; Fillion, M.; Hendzel, M. J.; Voelter, W.; Verdin, E. *J. Biol. Chem.* **2001**, *276*, 35826.
- Peart, M. J.; Smyth, G. K.; van Laar, R. K.; Bowtell, D. D.; Richon, V. M.; Marks, P. A.; Holloway, A. J.; Johnstone, R. W. *Proc. Natl. Acad. Sci. U.S.A.* **2005**, *102*, 3697.
- Karagiannis, T. C.; El-Osta, A. *Leukemia* **2007**, *21*, 61.
- Witter, D. J.; Harrington, P.; Wilson, K. J.; Fleming, J. C.; Kral, A. M.; Secrist, J. P.; Miller, T. A. submitted for publication. During the preparation of this manuscript, Methygene, Inc., disclosed a similar observation: Moradei, O. M.; Mallais, T. C.; Frechette, S.; Paquin, I.; Tessier, P. E.; Leit, S. M.; Fournel, M.; Bonfils, C.; Trachy-Bourget, M.-C.; Liu, J.; Yan, T. P.; Lu, A.-H.; Rahil, J.; Wang, J.; Lefebvre, S.; Li, Z.; Vaisburg, A. F.; Besterman, J. M. *J. Med. Chem.* **2007**, *50*, 5543.
- Benzamide **2** was originally designed for antiprotozoal (malaria) applications using total nuclear HDACs as a screening tool. Molecular modeling studies indicated that trichostatin A could overlay favorably with key elements of the apicidin pharmacophore: its ketone-containing side chain and indole moiety (similar analyses were performed using MS-275). Using modeling insights as guidance, rapid analog synthesis promptly yielded a series of potent hydroxamic acid derivatives. Incorporation of the *o*-hydroxy-benzamide moiety into this series as a metal chelating surrogate and further SAR development identified **2** which exhibited comparable intrinsic activity against total mammalian and protozoan nuclear HDACs. See: Meinke, P. T.; Liberator, P. H. *Curr. Med. Chem.* **2001**, *8*, 211.
- For enzyme assay procedure, see Ref. 7.
- For cell viability assay procedure, see Ref. 7.
- Wang, D.-F.; Wiest, O.; Helquist, P.; Lan-Hargest, H.-Y.; Wiech, N. L. *J. Med. Chem.* **2004**, *47*, 3409.
- Vannini, A.; Volpari, C.; Gallinari, P.; Jones, P.; Mattu, M.; Carfi, A.; De Francesco, R.; Steinkühler, C.; Stefania Di Marco, S. *EMBO J.* **2007**, *8*, 879.
- El-Beltagi, H. M.; Martens, A. C. M.; Lelieveld, P.; Haroun, E. A.; Hagenbeek, A. *Cancer Res.* **1993**, *53*, 3008.
- A solution of the inhibitor in 10% DMSO/45% PEG-400/45% water was administered once daily ip for up to 21 days.